

# The influences of partial saturation on cone penetration tests in silty gold tailings

Adrian Russell<sup>1</sup>, Thanh Vo<sup>2</sup>, Juan Ayala<sup>3</sup>, Yanzhi Wang<sup>1</sup>, David Reid<sup>3</sup>, and Andy Fourie<sup>3</sup>

<sup>1</sup>Centre for Infrastructure Engineering and Safety, School of Civil and Environmental Engineering, UNSW Sydney, NSW, Australia

<sup>2</sup>School of Engineering, The University of Warwick, Coventry, United Kingdom

<sup>3</sup>School of Civil, Environmental and Mining Engineering, The University of Western Australia, Perth, WA, Australia

**Abstract.** Laboratory-controlled cone penetration test results of a silty gold tailings in a variety of saturated and unsaturated states, obtained using two calibration chambers, are presented then interpreted using a state parameter-based approach. The research was conducted as part of the TAILLIQ project ([tailliq.com](http://tailliq.com)), funded by the Australian Research Council and six mining companies, and involving four Australian universities. Cone penetration resistances, which increase due to the presence of suction when the tailings are unsaturated, can be normalised using the initial mean effective stress to establish a relationship with the initial state parameter. The relationship is applicable to saturated and unsaturated conditions, as long as the presence of suction hardening as well as the influence of suction on the mean effective stress are accounted for, and as long as the cone penetrations occur under pseudo drained conditions. The relationships enable state parameters and void ratios to be back-calculated from normalised cone penetration resistances.

## 1 Introduction

The cone penetration test (CPT) is widely used to characterise tailings inside a tailings storage facility (TSF). There are many sections of the tailings which are unsaturated, including tailings above water levels, as well as tailings below water levels where embankment lifts have been constructed on top of desiccated surfaces ([1]), yet this partial saturation has not been addressed in the CPT correlations used. This makes interpreting CPTs in tailings somewhat unreliable and hinders ongoing efforts to reduce the number of TSF failures.

Account must be given to the suction ( $s$ ) present in an unsaturated tailings. Suction causes the particle contact forces to increase above what they would be when saturated or dry. The macroscopic effects are an increase in the effective stress. The contribution of suction to the effective stress may be denoted as  $\chi s$ , where  $\chi$  is the effective stress parameter ([2]). Also,  $s$  may harden the tailings making it stiffer and stronger. Suction hardening can be viewed as an upward  $s$ -dependant shift of the critical state line (CSL) in the  $e: \ln p'$  plane ([3]). Prior CPT studies (e.g. [4, 5, 6, 7]), show that  $s$  increases the cone penetration resistance,  $q_c$ , above what it would be for a saturated condition. Despite these studies no correlations have been developed which interpret the CPT data in a state parameter-based framework. The state parameter  $\psi$  [8] is a common measure of a tailings' state, being the vertical distance between the void ratio ( $e$ ) and the CSL in the  $e: \ln p'$  plane, with  $p'$  denoting the mean effective stress. This paper addresses that shortcoming. It summarises the results of CPTs performed in a silty gold tailings (from [9]) in saturated and unsaturated states. The CPTs were conducted under laboratory-controlled

conditions using two calibration chambers to establish correlations between  $q_c$  and state. Tailings properties, including water retention for different suctions, effective stresses and critical state lines were also obtained to assist with the correlation development. Extensions of established state parameter based correlations are shown.

## 2 Effective stress and water retention in unsaturated tailings

A suction  $s$  is present in an unsaturated tailings and causes the particle contact forces to increase above what they would be when saturated or dry. The macroscopic effects are increases in the stiffness of the tailings' skeleton and the effective stress.  $p'$  is defined as [10]:

$$p' = p + \chi s \quad (1)$$

where a prime symbol denotes the stress to be effective;  $p$  is the mean total stress in excess of pore-air pressure ( $u_a$ ) also referred to as the net stress;  $s$  is the difference between pore-air and pore-water pressure ( $s = u_a - u_w$ ); and  $\chi$  is 1 for saturated and 0 for dry conditions. To establish  $\chi$  it is necessary to consider how water is retained in the tailings. The relationship between degree of saturation ( $S_r$ ) and  $s$  is used, referred to as a water retention curve (WRC). For a given  $e$  the WRC comprises a main drying curve and a main wetting curve and many scanning curves. The main wetting and drying curves and scanning curves are idealized as being linear in the double logarithmic  $S_r$  versus  $s$  plane (Fig. 1).  $S_r$  on the main drying and wetting curves may be defined as [11]:

$$S_r = \begin{cases} 1 & \text{for } s \leq s_e \\ \left(\frac{s}{s_e}\right)^\alpha & \text{for } s \geq s_e \end{cases} \quad (2)$$

where  $\alpha$  is a constant and slope of the curves.  $s_e$  is the  $s$  separating saturated from unsaturated states. For a state on the main drying curve  $s_e = s_{ae}$ , where  $s_{ae}$  is the air entry suction. For a state on the main wetting curve  $s_e = s_{ex}$ , where  $s_{ex}$  is the air expulsion suction. Scanning curves have a slope of  $\beta$ . The WRC for a certain  $e$  can be made applicable to any other  $e$  through  $s_{ae}$  and  $s_{ex}$  using ([11]):

$$s_{ae} = C_1 e^{-D_s} \quad s_{ex} = C_2 s_{ae} \quad (3)$$

in which  $C_1$  is a positive constant with units of stress,  $C_2$  is a dimensionless constant and  $D_s$  is the fractal dimension of the particle size distribution.  $\chi$  may be defined as ([12]):

$$\chi = \begin{cases} 1 & \text{for } \frac{s}{s_e} \leq 1 \\ \left(\frac{s}{s_e}\right)^\Omega & \text{for } \frac{s}{s_e} \geq 1 \end{cases} \quad (4)$$

when the hydraulic state is located on the main wetting or main drying curve.  $\Omega$  is a negative material constant with a best fit value of -0.55. On a scanning curve  $\chi$  is:

$$\chi = \begin{cases} \left(\frac{s_{rd}}{s_{ae}}\right)^\Omega \left(\frac{s}{s_{rd}}\right)^\zeta & \text{for drying reversal } \left(\frac{s_{ex}}{s_{ae}}\right)^{\Omega-\zeta} s_{rd} \leq s \\ \left(\frac{s_{rw}}{s_{ex}}\right)^\Omega \left(\frac{s}{s_{rw}}\right)^\zeta & \text{for wetting reversal } s \leq \left(\frac{s_{ae}}{s_{ex}}\right)^{\Omega-\zeta} s_{rw} \end{cases} \quad (5)$$

where  $\zeta$  is a negative material constant. The relationship between  $\chi$  and  $s$  is shown in Fig. 1.

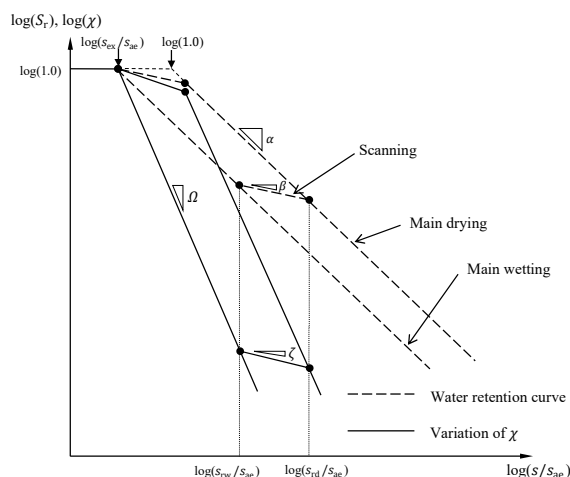


**Fig. 1.**  $S_r$  and  $\chi$  plotted against  $s/s_{ae}$  in double logarithmic planes.

### 3 Tailings properties

The gold tailings is a low plasticity sandy silt. Particles have a specific gravity  $G_s = 2.78$ . The particle size distribution is fractal with  $D_s = 2.618$ . The WRC is presented in Fig. 2, with key definitions overlaid. Triaxial testing revealed that the CSL may be defined (for  $p' < 2000\text{kPa}$ ) using

$$e = \Gamma - \lambda \ln p' \quad (6)$$

where  $\lambda = \lambda_{sat} = 0.036$  for  $SR = s/s_{ex} < 1$ ,  $\lambda = \lambda_{sat} + 4.5(SR^{0.004+0.015/SR} - 1)$  for  $SR > 1$ ,  $\Gamma = \Gamma_{sat} = 0.781$  for  $SR < 1$  and  $\Gamma = \Gamma_{sat} + (\lambda - \lambda_{sat})\ln(2000)$  for  $SR > 1$ . The CSLs for saturated conditions and  $SR = 50$  and  $SR = 150$ , and data points used to determine them are illustrated in Fig. 3.  $SR = s/s_{ex}$  is a suction ratio.

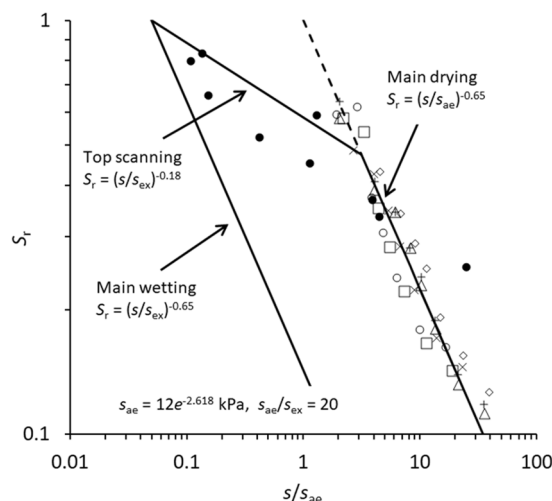


**Fig. 2.** WRC for gold tailings (solid symbols from filter paper tests, hollow/cross symbols from pressure plate tests).

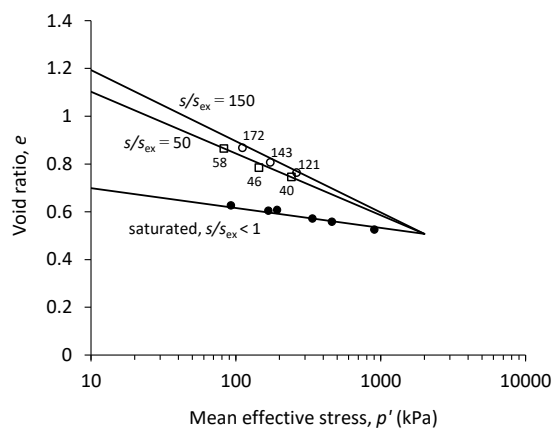


**Fig. 3.** CSLs for saturated and unsaturated gold tailings. Also shown are the end points of triaxial compression tests used to determine the line locations. Solid symbols for saturated conditions, hollow square and circle symbols are for constant suction conditions. Numbers next to the hollow symbols indicate  $SR = s/s_{ex}$ .

#### 4 CPT results and interpretation

CPTs were performed in two calibration chambers, one at The University of New South Wales (UNSW) and one at The University of Western Australia (UWA). Chamber details are in [13, 14]. The unsaturated tailings samples in the UNSW chamber had  $S_r$  that ranged from 0.20 to 0.61,  $e$  that ranged from 0.1 to 1.0 and  $v_a/v = \frac{e}{1+e}(1 - S_r)$  that ranged from 0.16 to 0.40. Since  $v_a/v > 0.15$  pseudo drained conditions prevail. A pseudo drained condition occurs when there is sufficient air in the pore space of the tailings such that the tailings skeleton deforms around a penetrating cone much like it would for penetrations during saturated drained conditions. The pressure of the pore air does not change significantly from the initial value, being atmospheric pressure. [15] found it was only for  $v_a/v < 0.15$  that a significant air pressure change and  $\chi s$  change occur during a fast loading event in silty tailings. Also, it is estimated that in practical settings involving tailings with considerable silt, the size of the cone would need to be at least 20 times larger than the maximum particle size (as was the case here) for there to be no size influences. A focussed research effort would be needed to confirm this.

The CPTs in the UWA chamber were on saturated tailings samples and involved cones with  $d_c = 6.4$  mm and 10 mm. Also,  $v_c = 0.2$  mm/s was used, slow enough to ensure drained conditions prevail. The  $e$  of the tested samples ranged from 0.57 to 0.72, i.e. slightly denser and looser than the saturated CSL where a liquefiable tailings typically transitions to one which can not liquefy.

Samples in both chambers were prepared by moist tamping.

When computing  $s$  and  $\chi s$  for the unsaturated cases from the known  $w$  and  $e$  it is assumed that the hydraulic state is located at the midpoint of a scanning curve. Equations (2) to (5) may then be adopted to compute  $s$  and  $\chi$ .

In the field normal seasonal cycles may see the state transition between wetting and drying, never reaching the main wetting or drying curve, instead remaining on a scanning curve the whole time. Unusual and prolonged wetting or drying processes, e.g. extreme floods or drought, may be exceptions that cause the hydraulic state to locate on a main wetting or drying curve. The direct evidence that the state usually stays on a scanning curve under normal climatic conditions is limited, although it is a view held by several in the unsaturated soil mechanics community. The study of [16], involving two years of monitoring data, does show that the hydraulic state of a loess soil slope is usually on a scanning curve.

The normalised cone resistance  $\frac{(q_c - p_0)}{p'_0} + 1$  (on a log scale) is plotted against  $\psi$  in Fig. 4. As  $\psi$  represents the vertical distance from the current state to the CSL in the  $e: \ln p'$  plane it depends on  $s$  and the  $SR$ -dependant locations of the CSLs.

Results of CPTs conducted in a soil or tailings under drained conditions exhibit a near-unique relationship

when plotted in this plane, as also observed here. It is of the form:

$$\frac{(q_c - p_0)}{p'_0} + 1 = \bar{k} \exp(-\bar{m}\psi) \quad (7)$$

in which  $\bar{k}$  and  $\bar{m}$  are positive dimensionless constants.

The results exhibit a unique relationship that may be defined by Equation (7) with  $\bar{k} = 47$  and  $\bar{m} = 6.6$ .

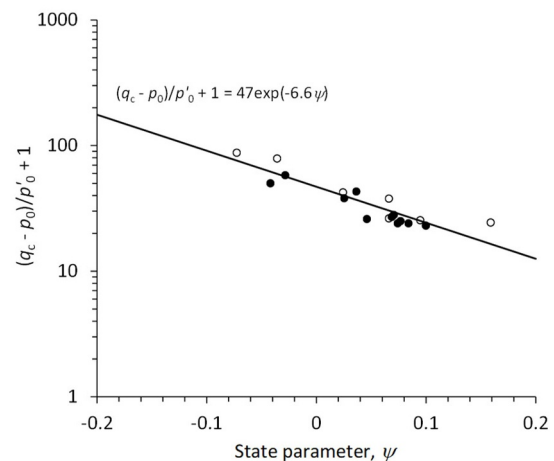


**Fig. 4.** Normalised cone resistance  $\frac{(q_c - p_0)}{p'_0} + 1$  against  $\psi$  for saturated and unsaturated gold tailings. Solid symbols for saturated tests, hollow symbols for unsaturated tests with  $v_a/v > 0.15$ .

Fig. 4 enables estimation of  $\psi$  from  $q_c$  provided that  $\chi s$  and  $p_0$  are known. For example, suppose  $q_c = 2600$  kPa was obtained for a certain depth from a CPT, where  $p_0 = 25$  kPa. It is further supposed that  $\chi s = 15$  kPa and doesn't change during the penetration. These values correspond to  $p'_0 = 40$  kPa and  $\frac{(q_c - p_0)}{p'_0} + 1 = 65.4$ . A value of  $\psi = -0.050$  is determined from Fig. 4. However, if suction is ignored and  $p'_0 = p_0 = 25$  kPa is incorrectly assumed, a value of  $\psi = -0.12$  would be determined from Fig. 4. Failure to account for suction influences in this example results in an error of -0.07 on the estimated  $\psi$ .

#### 5 An alternate presentation for field use

Gaining knowledge of  $e$  in an unsaturated tailings deposit is particularly useful as  $e$  is a property that would not change a lot if the tailings were to become saturated later, for example due to a rise in the water table as the tailings storage is heightened. A profile of  $e$  with depth in unsaturated tailings would be a useful output from a CPT sounding. The  $e$  profile can be combined with knowledge of the saturated CSL and used to determine a  $\psi$  profile in the tailings applicable to when it becomes saturated later. Sections that may become susceptible to liquefaction in the future can then be identified. The current  $\psi$  values, when the tailings are unsaturated, obtained from Fig. 4, depend on the current

$s$  and the  $SR$ -dependant locations of the CSLs through  $\Gamma$  and  $\lambda$ . While the current  $\psi$  is useful for short term strength and stability assessments, it would not assist with understanding how the tailings behave at a later time if they were to become saturated.

The relationship between  $\frac{(q_c - p_0)}{p_0} + 1$  and  $\psi$  enables  $e$  to be determined from  $q_c$  and  $p_0$ , as long as  $w$ ,  $\chi s$ ,  $s/s_{ex}$ ,  $\lambda$  and  $\Gamma$  are known as well. Specialised laboratory tests are usually required to determine the WRC, how  $s_{ae}$  and  $s_{ex}$  depend on  $e$ , the magnitude of  $\chi s$  for a given  $w$  and  $e$ , and how  $\lambda$  and  $\Gamma$  vary with  $s/s_{ex}$ , and are conducted for tailings only on very rare occasions.

Here, for the gold tailings, the corresponding relationships between  $q_c/p_0$  and  $e$ , for certain values of  $p_0$  and  $w$ , are plotted in Fig. 5. These relationships are useful to practicing engineers to obtain an estimate of  $e$ . Knowledge of  $\chi s$ ,  $s/s_{ex}$ ,  $\lambda$  and  $\Gamma$  is not required to apply them. The relationships are valid as long as  $v_a/v > 0.15$  and the hydraulic states are at the midpoints of scanning curves. The  $v_a/v > 0.15$  condition ensures pseudo conditions prevail in the tailings around the penetrating cone and the relationship in Fig. 4 applies. There is anecdotal evidence that, in unsaturated soils and tailings in the field, the hydraulic state is usually located somewhere between the main drying and wetting curve, so the midpoint assumption is a reasonable approximation to what is usually present.

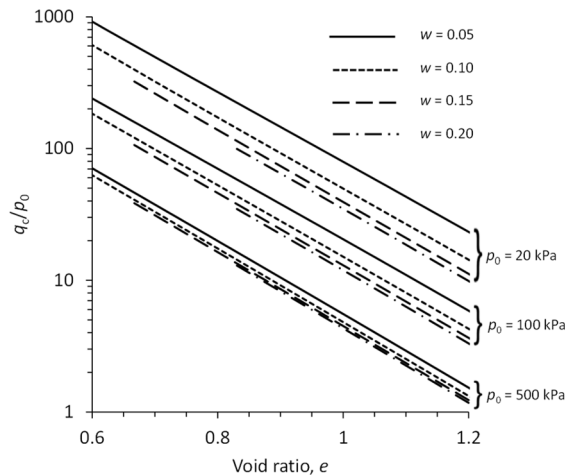


**Fig. 5.** The relationships between  $q_c/p_0$  and  $e$ , for certain values of  $p_0$  and  $w$  for the gold tailings, enabling estimation of  $e$ . The relationships apply when  $v_a/v > 0.15$  and the hydraulic states are at the midpoints of scanning curves.

Using the relationships in Fig. 5 requires knowledge of  $w$ , which is easily determined from samples taken from boreholes, and the total mean stress  $p_0$ , which may be estimated using an approximate unit weight, test depth and an assumption about how the horizontal stress relates to the vertical stress. The effective mean stress  $p'_0$  has been omitted, deliberately, from the normalised quantity  $q_c/p_0$  as it requires knowledge of  $\chi s$ .

Suppose  $q_c = 4500$  kPa was measured in unsaturated gold tailings at a depth of 7 m where  $w = 0.076$ . The total unit weight of the tailings at and above the test location is approximately  $\gamma = 16$  kN/m<sup>3</sup>. The vertical

total stress at the test depth is then  $\sigma_v = 112$  kPa. The horizontal total stress at the test depth is given by:

$$\sigma_h = K_0 \sigma_v + (K_0 - 1) \chi s \quad (8)$$

where  $K_0$  is the ratio between effective horizontal and vertical stresses. Assuming  $K_0 = 1 - \sin \phi'_{cs} = 0.434$  (using Jaky's equation) and  $\chi s = 10$  kPa then the mean total stress is  $p_0 = 66$  kPa. It follows that  $q_c/p_0 = 68.2$  and, from Fig. 5, leads to the estimated  $e$  being 0.825 (interpolating between the relevant relationships for certain  $p_0$  and  $w$  values). If the tailings were to become saturated later, with the phreatic surface being at the tailings surface, and no change to  $e$  occurred, then  $p'_0 = 41.8$  kPa (adopting  $\gamma = 19.4$  kN/m<sup>3</sup> for the saturated case) and  $\psi = 0.178$ .

For comparison, the relationships between  $q_c/p_0$  and  $e$  are plotted in Fig. 6 for when the hydraulic states are on the main wetting curves. Again the  $v_a/v > 0.15$  condition is required for validity. For a given  $w$ ,  $e$  and  $p_0$ , a smaller  $q_c$  applies compared to when the states are at the midpoints of scanning curves. In general,  $q_c$  is 1.7 to 2.0 times smaller for  $p_0 = 20$  kPa, 1.3 to 1.5 times smaller for  $p_0 = 100$  kPa, and 1.05 to 1.2 times smaller for  $p_0 = 500$  kPa.

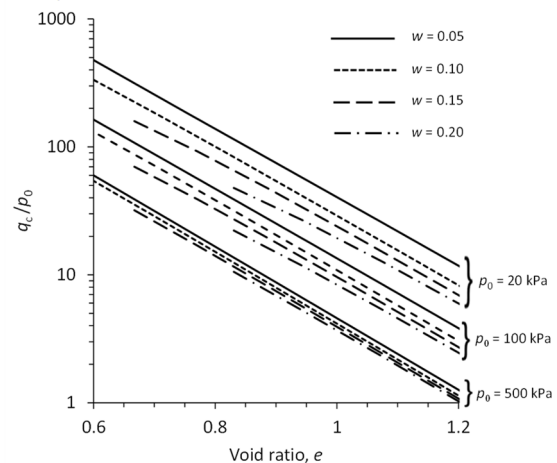


**Fig. 6.** The relationships between  $q_c/p_0$  and  $e$ , for certain values of  $p_0$  and  $w$  for the gold tailings, enabling estimation of  $e$ . The relationships apply when  $v_a/v > 0.15$  and the hydraulic states are on the main wetting curves.

## 6 Conclusion

An empirical expression relates the state parameter to a normalised cone penetration resistance for a tailings in saturated and unsaturated states. When unsaturated, as long as they are drier than a certain threshold, i.e.  $v_a/v > 0.15$ , cone penetration occurs under a pseudo drained condition, meaning  $\chi s$  remains (near) constant. The data may be interpreted once the effects of suction, in particular  $\chi s$ , are included in the effective stress. The interpretation enables direct estimation of  $\psi$ . Neglecting suction will lead to unconservative estimations of  $\psi$ . When saturated, however, slower than standard penetration velocities may be needed to ensure drained conditions prevail so that the relationships are the same as those observed for unsaturated conditions.

An alternate presentation may be formed in a plane that relates a normalised cone resistance to void ratio for a given moisture content and mean net stress. Its use does not require knowledge of suction, effective stress or the suction dependant locations of CSLs. It does, however, require an assumption about where the hydraulic state is located. Here that is taken to be the midpoint of a scanning curve, as that is thought to be a reasonable approximation for many real practical situations.

This work forms part of TAILLIQ (Tailings Liquefaction), which is an Australian Research Council (ARC) Linkage Project (LP160101561) supported by financial and in-kind contributions from Anglo American, BHP, Freeport-McMoran, Newmont, Rio Tinto and Teck. The TAILLIQ project is being carried out at The University of New South Wales, The University of South Australia, The University of Western Australia (lead organisation) and The University of Wollongong. We acknowledge the support and contributions of project personnel at each of the supporting organisations. The work also forms part of an ARC Future Fellowship (FT200100820) awarded to the first author at The University of New South Wales and that funding is gratefully acknowledged.

## References

1. A.B. Fourie, B.A. Hofmann, R.J. Mikula, E.R.F. Lord, P.K. Robertson, *Géotechnique* **51**, 7 (2001)
2. A.W. Bishop, *Teknisk Ukeblad* **106**, 39 (1959)
3. B. Loret, N. Khalili, *Mech. Materials* **34**, 2 (2002)
4. M. Pournaghiazar, A.R. Russell, N. Khalili, *Géotechnique* **63**, 14 (2013)
5. H. Yang, A.R. Russell, *Can. Geotech. J.* **53**, 3 (2016)
6. G.A. Miller, N.K. Tan, R.W. Collins, K.K. Muraleetharan, *Trans. Geotech.* **17**, B (2018)
7. C.T. Tang, R.H. Borden, M.A. Gabr, *J. Geotech. Geoenv. Eng.* **143**, 11, (2019)
8. K. Been, M.G. Jefferies, *Géotechnique* **35**, 2 (1985)
9. A.R. Russell, T. Vo, J. Ayala, Y. Wang, D. Reid, A.B. Fourie, *Géotechnique*, 10.1680/jgeot.21.00261, (2022)
10. A.W. Bishop, *Teknisk Ukeblad* **106**, 39 (1959).
11. A.R. Russell, *Géotechnique* **64**, 5 (2014)
12. N. Khalili, M.H. Khabbaz, *Géotechnique* **48**, 5 (1998)
13. M. Pournaghiazar, A.R. Russell, N. Khalili, *Can. Geotech. J.* **48**, 2 (2011)
14. J. Ayala, A.B. Fourie, D. Reid, *Géotech. Lett.* **10**, 4 (2020)
15. T. Vo, Y. Wang, A.R. Russell, *Géotechnique*, **72**, 3 (2022)
16. K. Yates, A.R. Russell, *Géotechnique*, 10.1680/jgeot.21.00042, (2022)